Mathematical Biosciences and Engineering

http://www.aimspress.com/journal/mbe

MBE, 22(8): 1931–1955.
DOI: 10.3934/mbe.2025070
Received: 25 February 2025
Revised: 15 April 2025
Accepted: 25 April 2025
Published: 19 June 2025

Research article

Modelling behavioural interactions in infection disclosure during an outbreak: An evolutionary game theory approach

Pranav Verma†, Viney Kumar† and Samit Bhattacharyya*

Disease Modelling Lab, Department of Mathematics, School of Natural Sciences, Shiv Nadar Institution of Eminence, Gautam Buddh Nagar 201314, India

† These authors contributed equally to this work.

* **Correspondence:** Email: samit.b@snu.edu.in.

Abstract: In confronting the critical challenge of disease outbreak management, health authorities consistently encourage individuals to voluntarily disclose a potential exposure to infection and adhere to self-quarantine protocols by assuring medical care (hospital beds, oxygen, and constant health monitoring) and helplines for severe patients. These have been observed during pandemics; for example, COVID-19 phases in many middle-income countries, such as India, promoted quarantine and reduced stigma. Here, we present a game-theoretic model to elucidate the behavioural interactions in infection disclosure during an outbreak. By employing a fractional derivative approach to model disease propagation, we determine the minimum level of voluntary disclosure required to disrupt the chain of transmission and allow the epidemic to fade. Our findings suggest that higher transmission rates and an increased perceived severity of infection may change the externality of the disclosing strategy, leading to an increase in the proportion of individuals who choose disclosure, and ultimately reducing disease incidence. We estimate the behavioural parameters and transmission rates by fitting the model to COVID-19 hospitalized cases in Chile, South America. The results from our paper underscore the potential for promoting the voluntary disclosure of infection during emerging outbreaks through effective risk communication, thereby emphasizing the severity of the disease and providing accurate information to the public about capacities within hospitals and medical care facilities.

Keywords: epidemic model; quarantine; evolutionary game theory; data-fitting; disease transmission

1. Introduction

In confronting critical challenges with disease outbreak management, especially during a pandemic, health authorities consistently advocate for voluntary adherence to disclosing a potential

exposure to infection and initiating self-quarantine protocols. Disclosing the potential exposure and subsequent quarantine not only helps public health to manage the crisis in terms of supplying medical care facilities, such as hospital beds and oxygen, to those who develop a severe infection, but also breaks the chain of infection transmission in the communities and reduces the cases. For example, managing the crisis during the COVID-19 outbreak remained challenging in spite of several measures such as lockdowns, quarantining healthy individuals, and mask mandates, especially in middle- and lower-income countries. The surge in cases in a short period of time overwhelmed public health systems, even to manage a small percentage of critical patients, thus straining medical facilities and hospital bed availability [1]. For instance, the Ministry of Health and Family Welfare (MoHFW) in India suggested that around 2.5% of patients needed intensive care at the beginning of the COVID epidemic. However, this might be underestimated due to incomplete reporting in some states [2]. As of June 28, 2020, the MoHFW reported 1055 dedicated COVID hospitals in India, with 177,529 isolation beds and 78,060 oxygen-supported beds. Additionally, there were 2,400 dedicated COVID Health Centres with 140,099 isolation beds and 51,371 oxygen-supported beds. However, this still left a considerable gap, with approximately 120,000 oxygen-supported beds available. It was estimated that 15% of patients, translating to about 1.5 million individuals in India, would require mild to moderate infection treatment with oxygen beds. Securing beds posed a significant challenge, as revealed by a Local Circles survey in April 2021 [3]. Only 13% of respondents successfully obtained an Intensive Care Unit (ICU) bed through the standard procedure, while the majority had to rely on personal connections. The survey indicated difficulties securing COVID-19 ICU beds for family and friends (see Figure 1). Later, to manage such overwhelmed situations, many centralized isolation and quarantine facilities were developed during the COVID-19 outbreak for patient observation and treatment [4, 5]. However, the decision to comply with such directives involves intricate strategic deliberations at the individual level, thereby weighing perceived benefits against the associated costs of disclosing prior exposure to infection and self-quarantine [6].

Researchers have increasingly utilized game-theoretic frameworks to explore the dynamic interplay between exposure disclosure, quarantine compliance, and disease containment [7]. During the COVID-19 outbreak, several game-theoretic models were developed to investigate the significance of quarantine (of healthy individuals) as a game-theoretic strategy and its impact on disease transmission [8, 9]. Martcheva et al. [8] introduced two models inspired by the COVID-19 pandemic, thereby incorporating elements of game theory, disease dynamics, human behaviour, and economics. A study by Premkumar et al. [10] delved into an evolutionary game theory model to examine an individual's behavioural patterns and to identify stable states. Alam and Tanimoto [9] emphasized the significance of promptly implementing multiple provisions to enhance disease containment efforts using game theory and human behaviour. Khazaei et al. [11] analyzed an integrated game-theoretic model to explore the dynamics of the public's compliance with social distancing measures and governmental influence and recommendations.

On the other hand, several fractional derivative models have been constructed to account for modelling memory effects and long-range dependencies to present in real-world epidemiological data [12, 13]. The foundational concepts of fractional derivatives were initially introduced by Oldham and Spanier [14], and more recent developments were discussed by Srivastava [15], further supporting the utility of this approach in complex systems. Moreover, Yunus et al. [12] developed a fractional order model to examine the impact of individual vaccinations on monitoring COVID-19

transmission. Wali et al. [13] introduced a novel numerical approach for the COVID-19 epidemic model based on the Atangana-Baleanu fractional order derivative in the Caputo sense to study vaccination efficacy. However, no study has considered disclosing an exposure to infection as an individual choice in the face of an outbreak and a limited availability of medical facilities. Understanding the interplay between individual strategies, medical facilities' availability, and their consequences on disease burden is an important challenge for public health policymakers.

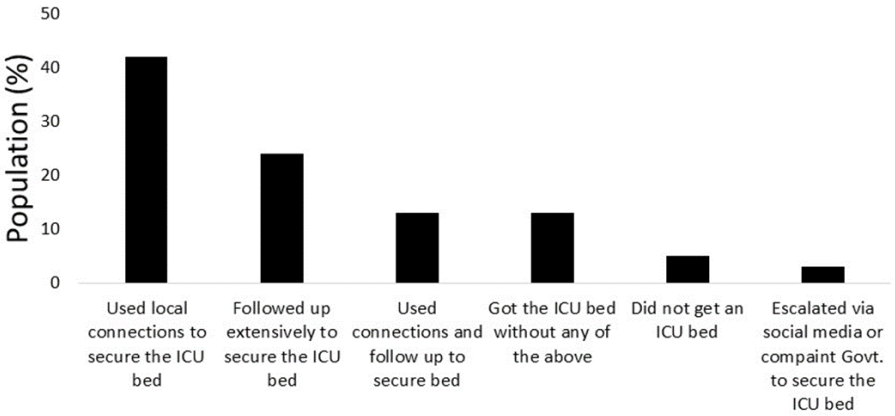

Figure 1. Impact of coronavirus (COVID-19) on securing ICU beds in hospitals across India as of April 2021 (Data source: https://www.statista.com/statistics/1231043/india-COVID-19-impact-on-securing-icu-beds-in-hospitals/).

This study explores the interplay between individual decision-making in disclosing an exposure and epidemiological factors by developing a game-theoretic model that utilizes fractional-order derivatives. We have identified the critical level of disclosure necessary for the epidemic to fade out. We simulate and explore how the disease transmission rate and interventions in public health, or the severity of the disease, influence an individual's decisions. According to our results, the population exhibits higher disclosure tendencies due to the combined impact of transmission and disease severity. Our analysis underscores the importance of infection disclosure as a strategic decision and its implications for illness control and the burden of hospitalization.

2. Model framework

2.1. Disease model

Here, we introduce the model given by Eq (2.1) to describe the disease propagation in the community. We divide the total population (N) into six distinct compartments: susceptible (S), exposed (E), infected (I), quarantined (Q), hospitalized (H), and recovered (R). This detailed compartmentalization is critical to capture the entire progression of the disease, from initial exposure through different stages of infection and treatment, while incorporating the behavioural response to public health interventions. In particular, by explicitly modelling these stages, our framework can evaluate how limitations in healthcare resources, such as hospital bed availability, directly influence the decision to self-quarantine. Figure 2 displays the schematic of the disease model, and Table 1

represents the variables used in the model. Tables 2 and 3 describe the parameters used in the model. In our model, we have adopted a fractional derivative approach to model the dynamics to incorporate memory effects and non-local interactions, which are critical to accurately capture the progression of an epidemic [16]. Unlike standard ordinary differential equations (ODEs), the fractional formulation accounts for the entire history of the system, thus allowing past states to influence the current dynamics. This is particularly relevant for modelling processes such as incubation periods and delayed behavioural responses, where the impact of previous exposures plays a significant role. Notably, Islam et al.'s [17] research demonstrated that fractional order derivatives (FODs) offer more flexibility in fitting empirical data and theoretically produce more accurate predictions despite the widespread use of ODEs for epidemic modelling. Moreover, when fitting our model to empirical data, the fractional derivative approach yielded a significantly improved fit compared to the standard ODE formulation (see Figure S4).

At the onset of the disease spread, a susceptible individual who comes in contact with an infected individual may or may not develop symptoms. We define the exposed state (E) as the subpopulation who were exposed to infected individuals in the community. The mean transmission rate of individuals from the S state to the E state is denoted by β_s, while the mean incubation rate of the force of infection from the E state to the I state is denoted by β_e.

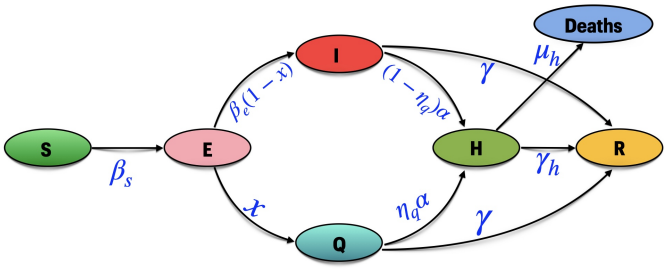

Figure 2. Schematic of the behaviour-prevalence model.

Furthermore, we assume that individuals aware of their exposure to infection may choose to disclose their exposure to the infection, voluntarily participate in self-quarantine, and subsequently move to the quarantined (Q) state. Those who do not opt for quarantine can spread the infection. In each of the I and Q states, individuals may develop severe symptoms and subsequently need to be hospitalized. In such a scenario, we assume that the hospitalizations from both states occur at an equal admission rate α, coupled with a public health preference factor η_q (discussed in the game-theoretical model in Section 2.2). Additionally, individuals in both these states may directly recover at a rate γ or may recover after being hospitalized at a rate γ_h. μ_h denotes the disease-induced mortality of hospitalized patients. Below, we have the epidemiological model equations using the FOD approach:

$$\begin{aligned}
\frac{d^\zeta S(t)}{dt^\zeta} &= \frac{-\beta_s(I+E)S}{N}, \\
\frac{d^\zeta E(t)}{dt^\zeta} &= \frac{\beta_s(I+E)S}{N} - xE - \beta_e(1-x)E, \\
\frac{d^\zeta Q(t)}{dt^\zeta} &= xE - \eta_q\alpha Q - \gamma Q,
\end{aligned}$$

$$\begin{aligned}
\frac{d^\zeta I(t)}{dt^\zeta} &= \beta_e(1-x)E - (1-\eta_q)\alpha I - \gamma I, \\
\frac{d^\zeta H(t)}{dt^\zeta} &= (1-\eta_q)\alpha I + \eta_q \alpha Q - \gamma_h H - \mu_h H, \\
\frac{d^\zeta R(t)}{dt^\zeta} &= \gamma I + \gamma Q + \gamma_h H,
\end{aligned} \tag{2.1}$$

which is subject to the following initial condition: $S(0) = S_0$, $E(0) = E_0$, $I(0) = I_0$, $Q(0) = Q_0$, $H(0) = H_0$, and $R(0) = R_0$. $\frac{d^\zeta S(t)}{dt^\zeta}$ represents a ζ order fractional derivative of the state $S(t)$ w.r.t time t. As we assume there is no reinfection of recovered individuals, and the total population is constant, we may exclude $R(t)$ from the model equations. Therefore, we present a reduced model that excludes the R compartment for analytical clarity and simplicity. Therefore, the reduced model is as follows:

$$\begin{aligned}
\frac{d^\zeta S(t)}{dt^\zeta} &= \frac{-\beta_s(I+E)S}{N}, \\
\frac{d^\zeta E(t)}{dt^\zeta} &= \frac{\beta_s(I+E)S}{N} - xE - \beta_e(1-x)E, \\
\frac{d^\zeta Q(t)}{dt^\zeta} &= xE - \eta_q \alpha Q - \gamma Q, \\
\frac{d^\zeta I(t)}{dt^\zeta} &= \beta_e(1-x)E - (1-\eta_q)\alpha I - \gamma I, \\
\frac{d^\zeta H(t)}{dt^\zeta} &= (1-\eta_q)\alpha I + \eta_q \alpha Q - \gamma_h H - \mu_h H,
\end{aligned} \tag{2.2}$$

which is subject to the following initial condition: $S(0) = S_0$, $E(0) = E_0$, $I(0) = I_0$, $Q(0) = Q_0$, and $H(0) = H_0$. x represents the percentage of exposed individuals who choose to disclose the exposure to infection and eventually be quarantined (see game-theoretic model in Section 2.2 for a description of x).

Table 1. Variables used in the model.

Variables	Description
N	Total population
$S(t)$	Number of susceptible individuals at time t
$E(t)$	Number of exposed individuals at time t
$I(t)$	Number of infected individuals at time t
$Q(t)$	Number of quarantined individuals at time t
$H(t)$	Number of hospitalized individuals at time t
$R(t)$	Number of recovered individuals at time t
$x(t)$	Fraction of exposed population opting to disclose exposure at time t

Table 2. Baseline parameters as described in the fractional model (2.2).

Parameters	Description
β_s	Mean disease transmission rate (per day)
β_e	Mean incubation rate (per day)
α	Rate of hospital admissions (per day)
μ_h	Mortality rate after hospitalization (per day)
ζ	Order of fractional derivative
γ	Recovery rate from infection (per day)
γ_h	Recovery rate of hospitalized patients (per day)

Table 3. Baseline parameters as described in the game model.

Parameters	Description
η_q	Preference by public health authorities to provide treatment facility
κ	Sampling rate in social learning (per day)
c_d	Per unit cost of disclosing infection
c_{nd}	Per unit cost of non-disclosing infection
p_S	Perceived probability of developing severe symptoms upon infection

2.2. Game-theoretical model

We classify this decision-making framework as a population game, where an individual's payoff is determined by their own behaviour as well as the collective behaviour of the community. The players are individuals exposed (E) to infection (I) (i.e., the strategy update takes place after exposure to infection in the context of disease dynamics). It is worth noting that individuals who choose to self-isolate are aware of their potential exposure to infection and voluntarily participate in self-quarantine. The decision-making is not based on the symptoms of infection. Let x ($0 \leq x \leq 1$) represent the fraction of the players who disclose their infection and opt for quarantine. It might be interesting to note that players of the present generation compete not only with players of the previous generation but also with players from past generations who have similar behaviours, since the individual choice relies on the current illness prevalence and availability of medical care and hospital facilities. We suppose that people imitate other individuals' behaviour, which is more likely for strategic decision-making in various social engagements. In particular, they adopt strategies from other members with a likelihood proportional to the projected payoff increase if the sampled individual's payoff is greater [18]. Individuals are presumed to choose their strategy based on the perceived benefits of disclosing the infection and quarantine.

Here we consider two strategies: *disclosing infection and opting for self-quarantine*, and *non-disclosing infection*. The perceived payoff of adopting a disclosure strategy is as follows:

$$p_d = -c_d(1 - \eta_q), \tag{2.3}$$

where c_d is the per-unit perceived cost of disclosing infection and isolation. We assume a disparity in medical care and hospital bed allocation between those who disclose exposure and self-quarantine and

those who do not [19]. In fact, many centralized isolation and quarantine facilities were established for patient observation and treatment during the COVID-19 outbreak [4, 5]. Such centralized facilities also play a major role in closely tracking the disease spread, thereby contributing to a more effective implementation of providing timely medical care to those who need it. As a result, these incentives that come along with quarantine become a lucrative choice for the exposed individuals, provided they participate by disclosing their exposure.

Hence, we introduce the parameter η_q to encompass all such preferences given by public health authorities (such as hospital beds and medical care) to individuals who disclose their infection and opt for quarantine. This parameter modifies the perceived payoff of disclosing according to the relationship. When $\eta_q = 0$, no preferential treatment is provided, and the complete disclosure cost c_d is incurred. Conversely, when $\eta_q = 1$, the benefit of public health intervention is maximized, thus nullifying the disclosure cost. This formulation captures the notion that more substantial public health support encourages individuals to disclose their exposure. The payoff of disclosing p_d is directly proportional to η_q in (2.3) and is based on the assumption that a greater availability of such public health preferences yields a larger payoff than otherwise. Our main intention is to analyze this factor's impact on the players' decision strategies during the disease outbreak. To do so, we simulate our model under both scenarios: when such preferences are available in varying magnitudes (given by (2.3)) and when they are not ($\eta_q = 0$).
The perceived payoff of adopting a non-disclosure strategy is as follows:

$$p_{nd} = -c_{nd} p_s f(H), \tag{2.4}$$

where c_{nd}, p_s are the perceived per unit cost of non-disclosing infection and the probability of developing severe infection, respectively. Individuals' perceptions of this factor are influenced by the community's current hospital admissions $H(t)$:

$$f(H) = \frac{H}{A + H}, \tag{2.5}$$

where A is the half-saturation coefficient. The cost of non-disclosing of infection increases as H increases. Therefore, the expected payoff gain upon changing the non-disclosing strategy to disclosing is as follows:

$$\Delta\mathcal{P} = p_d - p_{nd} = -c_d(1 - \eta_q) + c_{nd} p_s f(H). \tag{2.6}$$

All individuals are payoff maximizers who randomly sample other population members and adopt the strategy which provides them with the highest payoff. Thus, the time evolution of the frequencies of the disclosure strategy for an imitation game is as follows:

$$\frac{d^\zeta x(t)}{dt^\zeta} = \kappa x(1 - x)(-c_d(1 - \eta_q) + c_{nd} p_s f(H)). \tag{2.7}$$

Here, κ is the sampling rate in social learning. Note that (2.6) is similar to the replicator equation in evolutionary game theory [18, 20].

2.3. Coupled disease game-theoretic model

By combining the game-theoretic model (Eq 2.7) with epidemiological model (2.2), we have the following:

$$\begin{aligned}
\frac{d^{\zeta}S(t)}{dt^{\zeta}} &= \frac{-\beta_s(I+E)S}{N},\\
\frac{d^{\zeta}E(t)}{dt^{\zeta}} &= \frac{\beta_s(I+E)S}{N} - xE - \beta_e(1-x)E,\\
\frac{d^{\zeta}Q(t)}{dt^{\zeta}} &= xE - \eta_q\alpha Q - \gamma Q,\\
\frac{d^{\zeta}I(t)}{dt^{\zeta}} &= \beta_e(1-x)E - (1-\eta_q)\alpha I - \gamma I,\\
\frac{d^{\zeta}H(t)}{dt^{\zeta}} &= (1-\eta_q)\alpha I + \eta_q\alpha Q - \gamma_h H - \mu_h H,\\
\frac{d^{\zeta}x(t)}{dt^{\zeta}} &= \kappa x(1-x)\Big(-c_d(1-\eta_q) + c_{nd}p_s f(H)\Big),
\end{aligned} \tag{2.8}$$

which is subject to the following initial condition:

$$S(0) = S_0, E(0) = E_0, I(0) = I_0, Q(0) = Q_0, H(0) = H_0, x(0) = x_0.$$

We evaluate and computationally simulate this model (Eq 2.8) to learn how changing behavioural and epidemiological characteristics affect the dynamics of disease prevalence.

3. Results

Since our model incorporates the strategies of disclosure ($x \neq 0$) and non-disclosure ($x = 0$), we compute the reproduction numbers in each case by evaluating the Jacobian of our system at the respective equilibrium points. The results obtained in each case are given below. A detailed calculation for the same is provided in the Appendix.

- The basic reproduction number R_0 at $x = 0$ is given by the following:

$$R_0 = \beta_S\left[\frac{1}{\beta_e} + \frac{1}{\Big((1-\eta_q)\alpha + \gamma\Big)}\right]. \tag{3.1}$$

- Whereas, the control reproduction number R_c when $x \neq 0$ is given by the following:

$$R_c(x) = \frac{\beta_s}{(x + \beta_e(1-x))}\left[1 + \frac{\beta_e(1-x)}{\Big((1-\eta_q)\alpha + \gamma\Big)}\right]. \tag{3.2}$$

We compute the threshold proportion of individuals x_c required to disclose their exposure, thus ensuring that the infection in the population completely dies out since, in this case, $R_c < 1$, making the disease-free equilibrium state stable. This threshold is given by the following:

$$x_c > \frac{\Big((1-\eta_q)\alpha + \gamma\Big)(\beta_s - \beta_e) + \beta_s\beta_e}{\beta_s\beta_e + (1-\beta_e)\Big((1-\eta_q)\alpha + \gamma\Big)}. \tag{3.3}$$

To examine how disease dynamics vary with the proportion of individuals choosing to disclose their infection, we treat x as a parameter for the time being and plot R_c using Eq (3.2) against various other parameters, such as the following: β_s (the transmission rate), η_q (public health preference in providing hospital beds), and α (rate of hospital beds in the community) (Figure 3). This figure clearly shows that higher values of x reduce the force of infection in the transmission of the disease (Figure 3(a)). Additionally, the higher availability of hospital beds in the community or even a relatively low preference in accessing hospitals among individuals with disease will die out immediately with a lower proportion of disclosing (Figure 3(b),(c)). This happens because the infected individuals, once hospitalized, are isolated, which reduces the transmission. This indicates that a greater supply of beds in the community might help reduce the transmission of infection. Now, we simulate the model using several parameters under baseline values to analyze the impact of disclosing infection on the dynamics of disease spread.

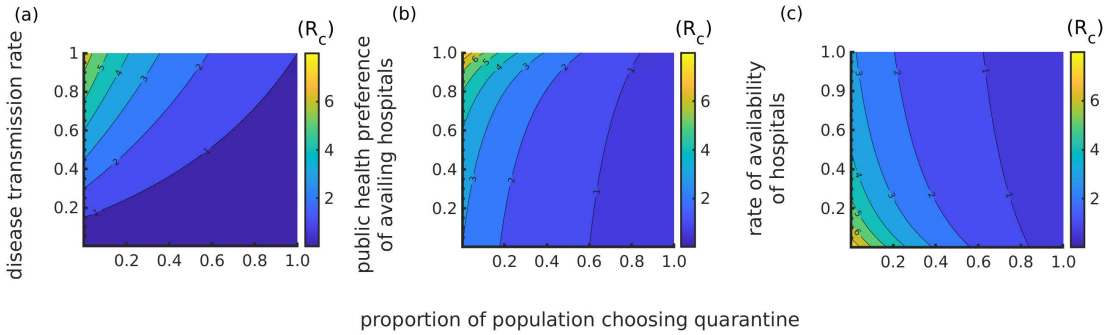

Figure 3. Control reproduction number (R_c) of the model for different values of $x : 0 < x \leq 1$ on the x-axis and (a) $0 < \beta_s < 1$ (b) $0 \leq \eta_q \leq 1$ (c) $0 \leq \alpha \leq 1$ on the y-axis.

4. Numerical simulation

We simulated the fractional differential equation (FDE) model (2.8) with the values of parameters described in Table 4. We assume an initial population size of $N = 50100$, with initial population distributions as follows: $E(0) = 0$; $I(0) = 100$; $Q(0) = 0$; $H(0) = 0$; $R(0) = 0$; and $x(0) = 0.15$. Most of the parameter values are chosen for the purpose of simulating the solutions of the FDE model, while the other values are appropriately cited from the literature.Numerical solutions for the FDE system are provided by the Adams-Bashforth-Moulton scheme, as described in the supplementary section. All computations and simulations were performed in Python by developing the entire code of the numerical scheme and applying it to our model. The results were compressed into CSV files and transferred to MATLAB for higher-resolution images, and all the corresponding plots were generated.

Table 4. Baseline values (or ranges) of the parameters used for the numerical simulations of the disease model (2.8).

Parameter	β_s	β_e	η_q	α	μ_h	ζ	γ	γ_h	κ	c_d	c_{nd}	p_S
Values/Ranges	0.6	0.3	(0–1)	(0–1)	0.3	0.9	0.1	0.071	(0–1)	(0–1)	(0–1)	(0–1)
Reference	[21]	[22]			[23]	[24]	[25]	[26]				

4.1. Impact of the rate of disease transmission and public health intervention on disease prevalence

The transmission rate of infection (β_s) and disease burden are important factors behind an individual's decision to adopt quarantine [27]. Figure 4 depicts the proportion of individuals in different compartments for sample values of β_s. A relatively small value of $\beta_s = 0.2$ would mean a smaller fraction of individuals moving to the exposed compartment daily, which subsequently leads to fewer infections, quarantines, and hospitalizations (Figure 4(a)–(c)). Alternatively, for a larger value of $\beta_s = 0.8$, the force of infection increases, which causes an increase in the number of individuals in all compartments (Figure 4(a)–(c)). There are two important observations in this simulation. The first is the stark difference in the transmission profile of infection in the presence and absence of disclosing options (Figure 4(a), dotted lines). The cumulative difference between these two profiles indicates that disclosing an exposure to infected neighbours may help reduce infection transmission by improving hospital bed management or by eventually isolating them from the general population, thus lowering the risk of infection transmission. The second observation is that the proportion of disclosing individuals at $\beta_s = 0.2$ is significantly lower than the cases when β_s is higher, since more exposed players are present in the latter (Figure 4(d)). Due to the high population in the infected and quarantined compartments for $\beta_s = 0.8$ (Figure 4(a),(b)), the probability of acquiring a severe disease is high. Consequently, a large hospitalized population can be seen (Figure 4(c)). Hence, the burden of surrounding infections directly influences this decision strategy. As a result, people choose to disclose their exposure.

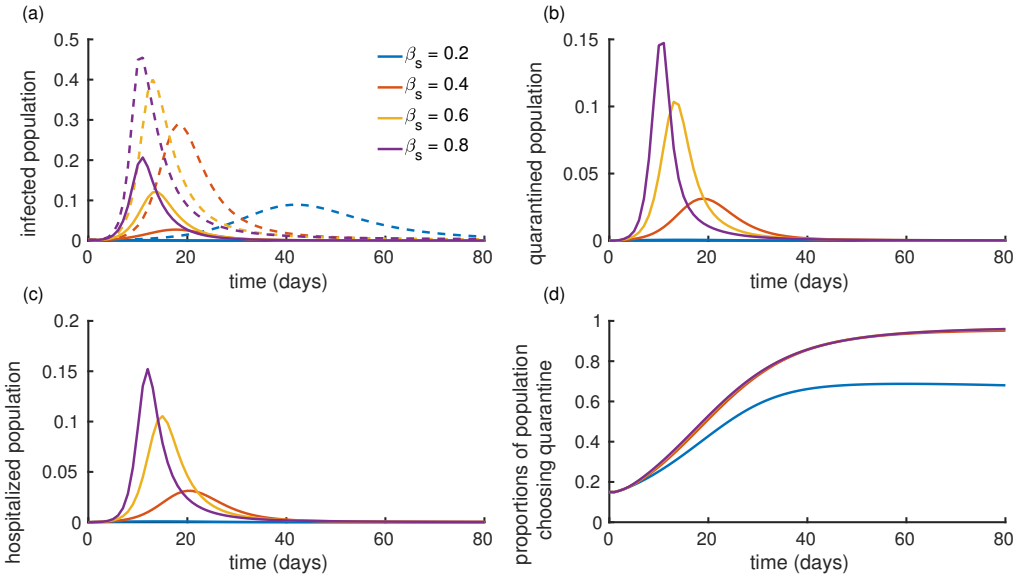

Figure 4. The dynamics of different trajectories of the model for various values of disease transmission rates, β_s: (a) infected population, (b) quarantine population, (c) hospitalized, and (d) proportion x of individuals who choose to disclose their infection, with $\kappa = 0.5$, $A = 10$, and $p_s = 0.8$. In Figure (a), the dotted line indicates the dynamics of the infected population when no individual chooses to disclose exposure (i.e., $x = 0$). These comparative trajectories underscore the importance of the decision game on the infection burden. The proportion of the individuals in each compartment is calculated as the number (infected, quarantined and hospitalized) in the compartment divided by the total population over time.

One of the public health measures during the COVID-19 epidemic was to provide priority access to hospital facilities for people who voluntarily entered quarantine. Figure 5 shows the impact of varying the public health preference factor η_q on the disease burden. A higher value of η_q works as an incentive of preference for the exposed individuals to choose quarantine, since it indicates a higher probability of getting hospital facilities. On the other hand, a lower η_q discourages quarantine, as seen in Figure 5(d). However, a similar trend is not reflected in the population of the Q compartment (Figure 5(b)) since individuals are also moving from the Q compartment to the H compartment at a higher rate for greater values of η_q. Additionally, the number of infections still remain high (Figure 5(a)), as higher η_q values decrease the chances for an infected individual to get a hospital facility, since they do not choose the strategy of disclosure. Of course, disclosing the exposure with and without shows a similar difference as earlier (Figure 4). This analysis indicates important information for public health policymakers: more hospital facilities for individuals who choose to be quarantined may not reduce the burden of non-disclosing infected individuals in the population to a great extent, which causes a larger contribution to the force of infection.

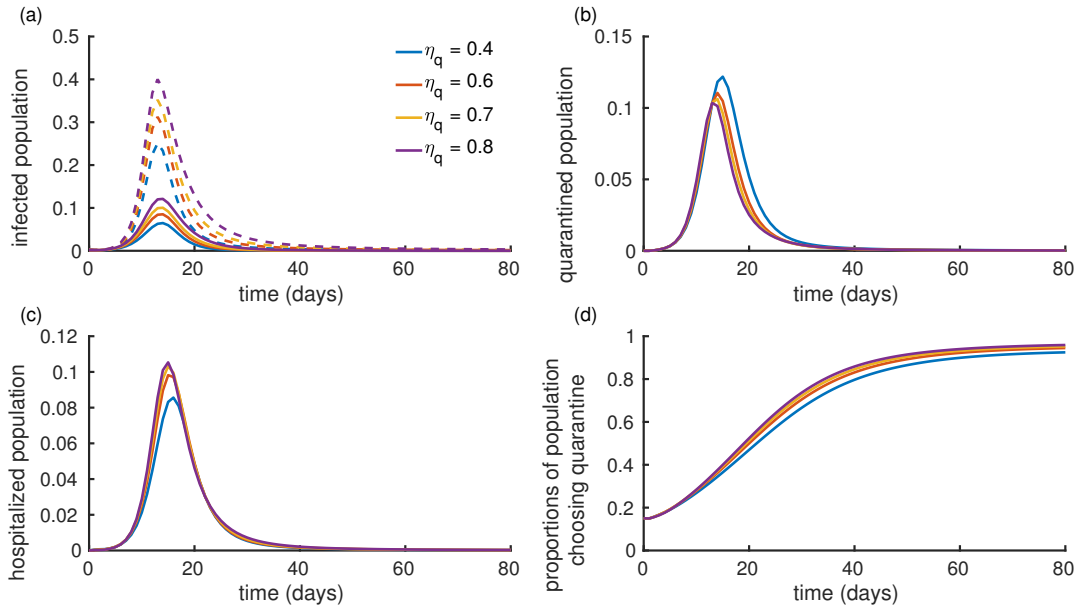

Figure 5. The dynamics of disease component for different values of public health preferences to treatment facilities (η_q): (a) infected population, (b) quarantine population (c) hospitalized, and (d) proportion x of individuals who choose to disclose their infection, with $\kappa = 0.5$ and $p_s = 0.8$. In Figure (a), the dotted lines indicate the dynamics of the infected population when no individual chooses to disclose exposure (i.e., $x = 0$).

Despite these results, the disease may be controlled by a combination of disease prevalence, burden, and public health initiatives. The combined influence of these two significant epidemiological factors on the cumulative new entries of each compartment is summarized in Figure 6. As previously observed, greater β_s values increase the disease burden, which results in a larger entry of individuals into the infected (I) compartment. However, in this case, the cumulative burden remains high irrespective of the values of η_q, since the new infections do not directly depend on η_q. This is per our model framework (Figure 4(a)). Since the new hospitalizations depend on η_q, higher values of β_s would imply a greater

movement of infected and quarantined individuals into the hospitalized compartment based on public health preferences. Consequently, hospitals will accommodate the greatest number of patients possible (Figure 6(c)). For $\eta_q \geq 0.899$ and $\beta_s \geq 0.5456$, the number of individuals entering quarantine is very high (Figure 6(b)) because, for the same values, the cumulative exposed population is very large.

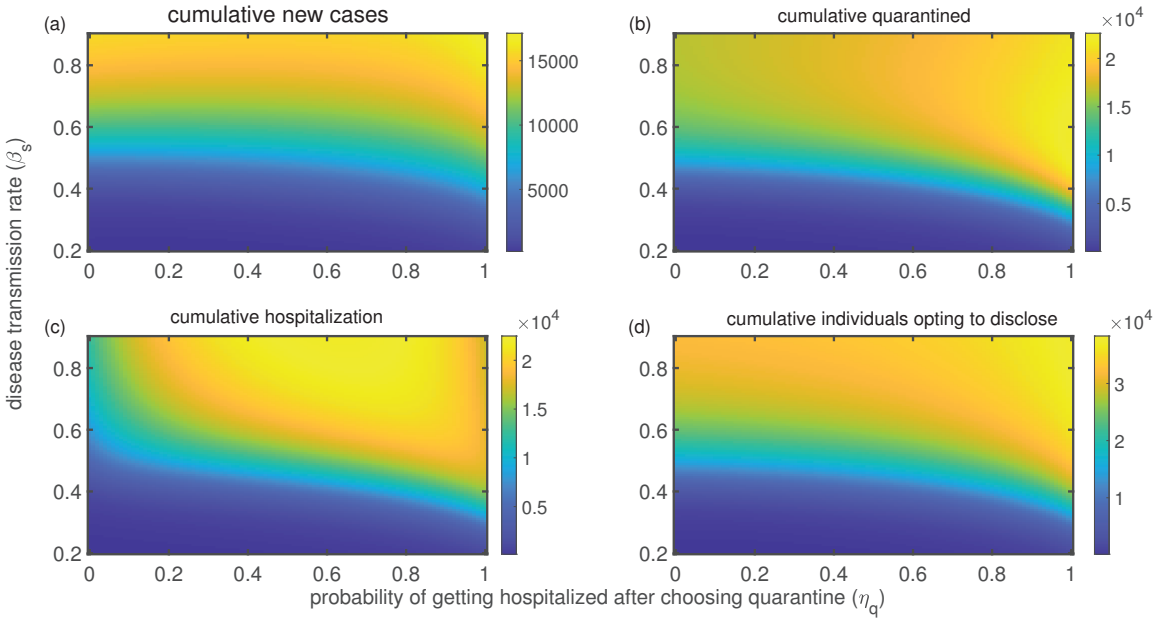

Figure 6. Cumulative population of (a) new cases, (b) quarantined, (c) hospitalization, and (d) individuals opting to disclose; as a function of the probability of getting hospitals after choosing quarantine (η_q) and transmission rate (β_s).

Additionally, we analyzed the difference between the baseline payoff of disclosure and the new payoff of disclosure without $1 - \eta_q$ to figure out the importance of public health measures (Figures 6 and S1). The cumulative new infections with our baseline payoff is $\approx 1.5 \times 10^4$ for $\eta_q \geq 0.8$ and $\beta_s \geq 0.7$ (Figure 6(a)); however, without $1 - \eta_q$, public health intervention does not affect the decision strategy, which leads to a greater cumulative infection that mainly varies due to β_s (Figure S1). Public health efforts may help control the disease if there is a high transmission rate. A similar trend in the cumulative quarantines can be seen in Figures 6(d) and S1(d) due to the interplay of these factors.

Our research suggests that the public health intervention of providing hospitals for quarantine has a favourable effect on the quarantine and hospital burden if the disease transmission rate is high in the community. Additionally, this can help reduce the prevalence of disease in the population. During a pandemic, public health agencies may implement measures that mitigate the effects of the disease on the general population.

4.2. Influence of incubation rate and probability of perceived severity on the disease

The rate of developing disease (β_e) after exposure to infection may play a certain role in disease dynamics. In Figure 7(a), a low value of $\beta_e = 0.2$ corresponds to a lesser contribution to the infected class, while a higher value of $\beta_e = 0.5$ would mean a greater contribution. Different values of β_e do not affect the decision strategy of disclosing the infection at the onset of the disease since the

replicator Eq (2.7) is independent of β_e. This is seen in Figure 7(d)). However, a change in the proportion of quarantined individuals still occurs, as reflected in Figure 7(b). This is because the number of individuals in the exposed compartment is initially constant for a fixed value of β_s. Then, based on non-disclosure, individuals move into the infection compartment at the rate of β_e, which leaves a fraction of individuals to move into quarantine by disclosing. Therefore, a lower value of $\beta_e = 0.2$ would correspond to an increase in the number of individuals deciding to move into quarantine, as shown by the blue curve in Figure 7(b). A change in the quarantined population also occurs due to the exit of individuals into the hospitalized and recovered compartments, as given by our model. Adopting a quarantine approach is heavily influenced by the relative probability of perceived severe symptoms after getting an infection. Figure 8 shows the interplay of disease severity and quarantine for different values of p_s. When the perceived probability of severity is very high (i.e., $p_s = 1$), more individuals prefer to adopt quarantine by disclosing their infection (Figure 8 (d),(b)). This simultaneously leads to a lesser proportion of individuals non-disclosing and hence moving into the infected compartment (Figure 8(a)). However, the number of hospitalizations remains unaffected in any scenario of severity, as seen in Figure 8(c), since the availability of hospital beds relies on η_q, and has no direct dependence on this probability. Overall, these results show that the infection rate influences the number of people in quarantine but does not affect the fraction of people choosing quarantine at any given time. However, if the surrounding individuals have a greater probability of developing a severe illness, then the proportion of people who can make decisions dramatically shifts through this perception. Our findings may prompt public health officials to take action in response to the outbreak by ordering more isolation units to be built.

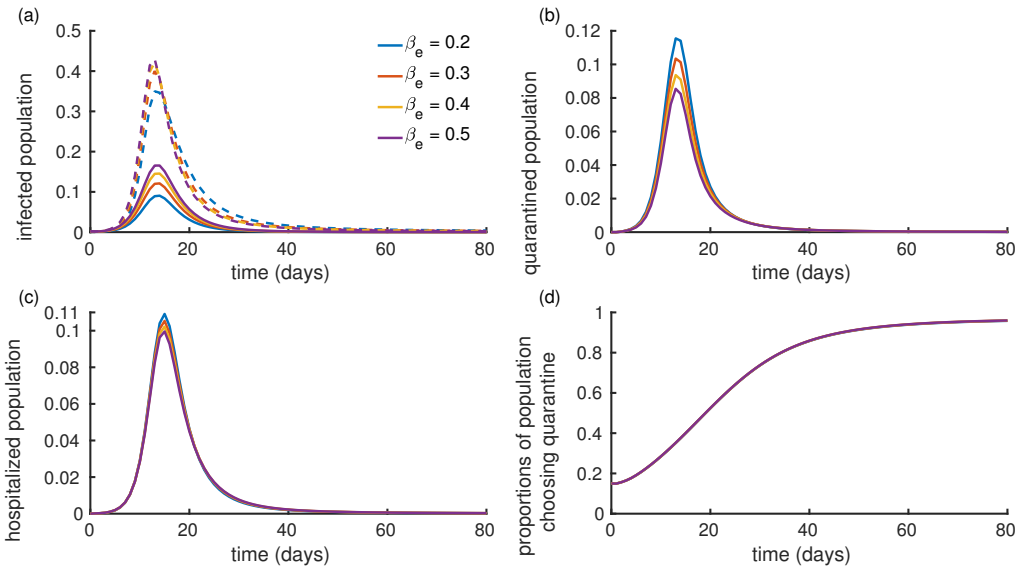

Figure 7. The dynamics of different trajectories of the model: (a) infected population, (b) quarantine population, (c) hospitalized, and (d) proportion x of individuals who choose to disclose their infection for different values of incubation rate (β_e). Here, $\kappa = 0.5$ and $p_s = 0.8$. In Figure (a), the dotted lines indicate the dynamics of the infected population when no individual chooses to disclose exposure (i.e., $x = 0$).

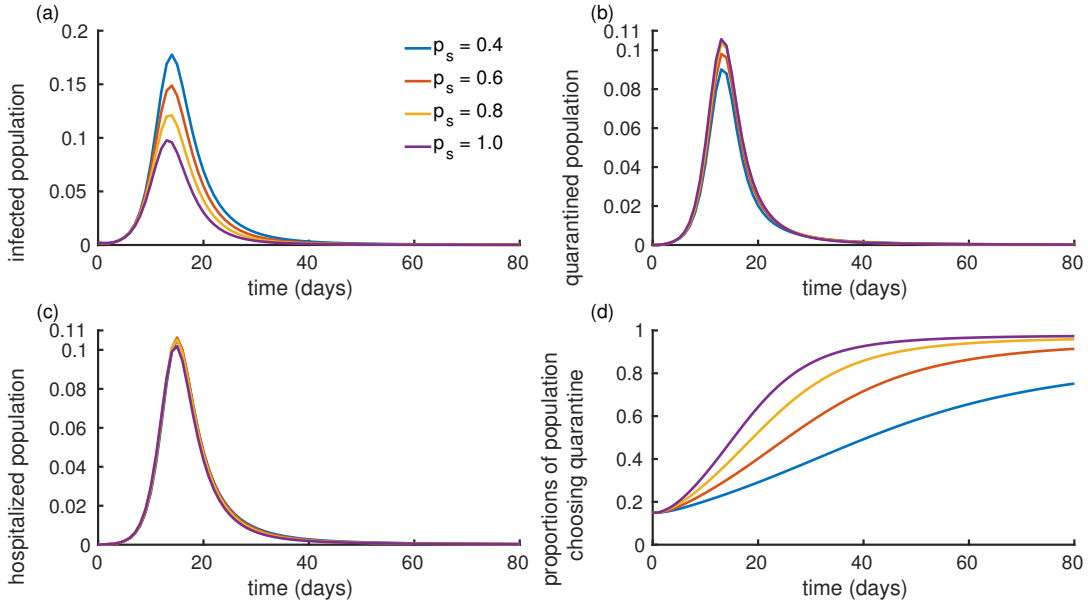

Figure 8. The dynamics of different trajectories of the model: (a) infected population, (b) quarantine population, (c) hospitalized, and (d) proportion x of individuals who choose to disclose their infection for different perceived probabilities of developing severe symptoms upon infection (p_s). Here, $\kappa = 0.5$.

4.3. Impact of the perceived probability of severity with preference by public health authorities to provide treatment facilities

Figure 9 summarizes the simultaneous effect of p_s and η_q on the cumulative new infections and hospital burden. For $p_s \leq 0.2$, higher values of η_q indicate that a large proportion of the population will opt for quarantine per day (Figure 9(d)). As the value of p_s rises, people will fairly play with the strategy and make decisions to maximize their payoffs. For $p_s \geq 0.8$ and $\eta_q \geq 0.9$ (Figure 9(d)), a large fraction of the population will engage in the decision-making process, which results in a greater inflow of individuals opting to quarantine (Figure 9(b)). Simultaneously, the inflow of infections reduces due to non-disclosure (Figure 9(a)). The burden of new hospitalizations also shrinks, as anticipated, when a significant portion of the public participates in the decision-making process (Figure 9(c)). Therefore, when $p_s \leq 0.2$ and $\eta_q \leq 0.6$ (Figure 9(c)), a significant portion of the population is hospitalized. Concurrently, p_s has a greater influence on the payoff (Figure 9(d)).

Additionally, we analyzed the difference between the baseline payoff and the new payoff of the disclosure without $1 - \eta_q$ to determine the importance of public health measures (Figures 9 and S2). When η_q is considered in our model, it mimics how public health interventions reduce the disease burden, whether or not the condition becomes severe. Based on our research, we hypothesize that the perceived severity of the illness is one of the main drivers of the increase in hospitalizations seen during the pandemic. If the public health benefits are greater for the quarantined population, then a large proportion will be involved in switching to disclose an exposure. Understanding the true extent of the infection and effective public health messaging can motivate people to opt for quarantine.

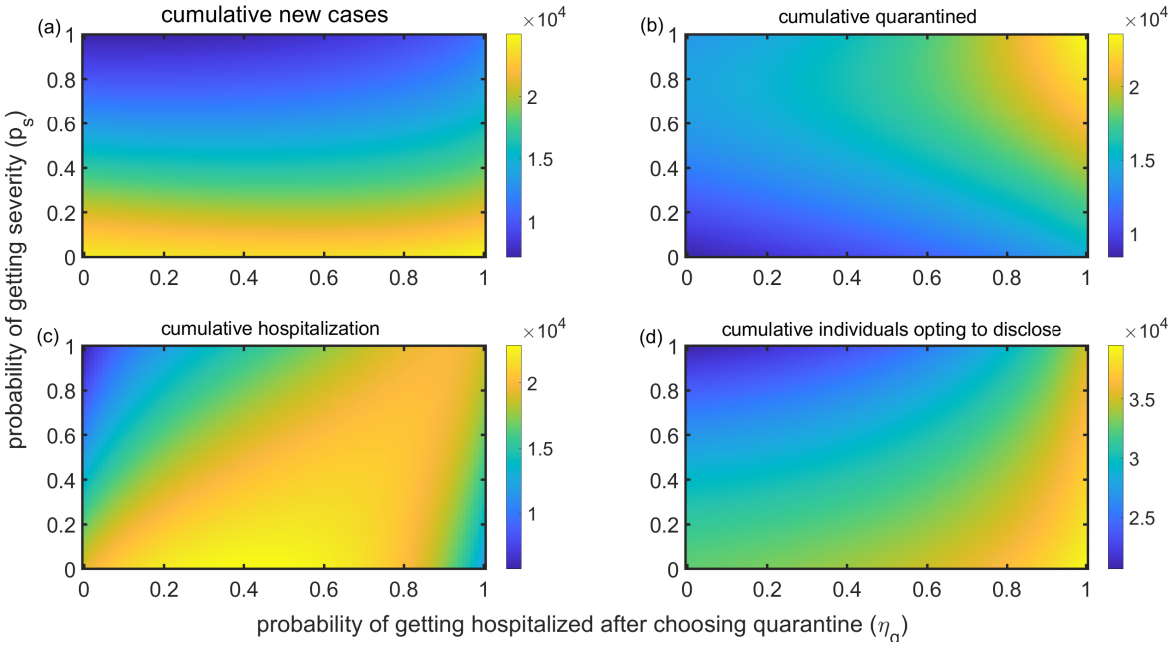

Figure 9. Cumulative population of (a) new cases, (b) quarantined, (c) hospitalization, (d) individuals opting to disclose; as a function of preference by public health authorities to provide treatment facility (η_q) and probability of getting severity (p_s).

4.4. Parameter sensitivity analysis

To assess the robustness of outcomes from our model and identify the most influential parameters driving the epidemic dynamics, we computed the Partial Rank Correlation Coefficients (PRCC) and corresponding p-values for important disease and behavioural parameters (see Table S3). The PRCC analysis identifies specific parameters which have a powerful influence on the model output. In particular, the disease transmission rate (β_s) and the incubation rate (β_e) exhibit PRCC values above 0.91, which indicate that even slight variations in these parameters lead to significant changes in the predicted epidemic dynamics (Figure 10). Similarly, the non-disclosure cost (c_{nd}) and the perceived probability of developing severe symptoms (p_s) are highly influential, as indicated by their strong negative correlations (with PRCC values around -0.92) (Figure 10). Parameters such as the public health intervention parameter (η_q) and the order of the fractional derivative (ζ) show moderate sensitivities, which suggest that while they affect the system, their impact is less pronounced compared to the primary epidemiological parameters. The cost of disclosing (c_d) demonstrates a relatively low sensitivity, which indicates that the model predictions are less sensitive to its variation.

This sensitivity analysis not only reinforces the robustness of our model but also supports our motivation: we can better inform public health strategies by accurately identifying the key drivers of disease transmission and behavioural response. Specifically, the high sensitivity of β_s and β_e underscores the importance of controlling transmission and managing the incubation process. At the same time, the significant influence of c_{nd} and p_s highlights the critical role of behavioural factors in epidemic outcomes. These insights underscore the necessity for targeted interventions and precise

parameter estimations in epidemic control.

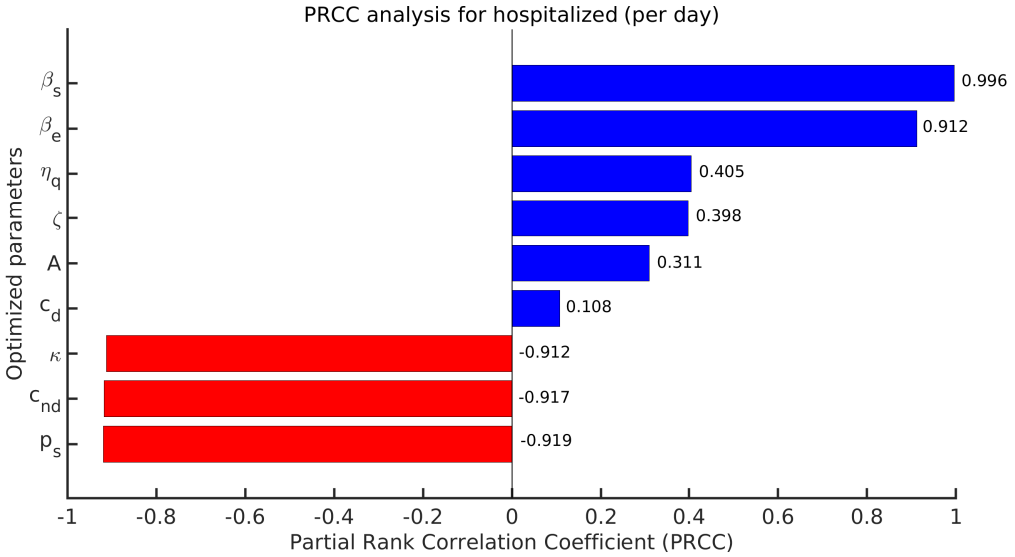

Figure 10. Figure shows the partial rank correlation coefficient (PRCC) analysis of the optimized model parameters. We have used latin hypercube sampling (LHS), considering 10,000 samples with a model simulated for 80 days. PRCC was calculated from the cumulative prevalence of the outbreak.

4.5. Data implementation, parameter estimation and scenario analysis

We used historical hospitalized cases during COVID-19 from Chile, South America to estimate the parameters in our model (2.8). The total population of Chile was 19.6 million. We considered daily hospitalized cases during the period from April to September 2020. Since the model does not account for vaccination, we chose the time period of the data as the pre-vaccination period. The data set was acquired through the *Our World in Data* [28]. We mainly estimate the freedom of information (FOI) parameters (such as η_q which can be accessed in the form of hospital bed availability and treatment priority information via public health portals) and the behavioral parameters (Table 5) denoted by Θ_e:

$$\Theta_e = \{\beta_s, \beta_e, \eta_q, c_d, c_{nd}, \kappa, A, p_S, \zeta\}.$$

Other parameters were kept fixed and were mainly obtained from the literature (see Table 6). We used the least squares approximation (LSA) approach to estimate the best parameters to explain the pattern of the outbreak. Additionally, we used the Monte Carlo approach with 10,000 samples and LHS sampling to compute the confidence interval [29, 30]. Figure 11 shows the 95% confidence interval (shaded region) together with the observed hospitalization data (black dots) and the estimated trajectory (red line). The strong alignment between the model and data suggests that our approach captures the key dynamics of daily hospitalizations, especially the peak timing and peak size.

Table 5. Estimated parameter values and confidence interval for model fitting to daily hospitalizations in Chile.

Parameters	Description	Optimized values (unit)	95% Confidence Interval
β_s	Mean disease transmission rate	0.262849 (per day)	[0.250, 0.276]
β_e	Mean incubation rate	0.97278 (per day)	[0.924,1]
η_q	Preference by public health authorities	0.45296	[0.430,0.476]
ζ	Order of fractional derivative	0.84552	[0.803,0.888]
κ	Sampling rate in social learning	0.016914 (per day)	[0.016, 0.018]
A	Half saturation coefficient	545.976	[519,573]
c_d	Per unit cost of disclosing infection	0.09425	[0.090,0.099]
c_{nd}	Per unit cost of non-disclosing infection	1.5053	[1.430,1.581]
p_S	Probability of developing severity upon infection	0.918087	[0.872, 0.964]

Table 6. Fixed parameter values (non-optimized) in Θ_f for data fitting of daily hospitalizations in Chile.

Parameters	Description	Values (per day)	ref.
α	Rate of hospital admissions	0.016	[31]
γ	Recovery rate from infection	0.1	[25]
γ_h	Recovery rate of hospitalized patients	0.067	[26]
μ_h	Mortality rate after hospitalization	0.011	[32]

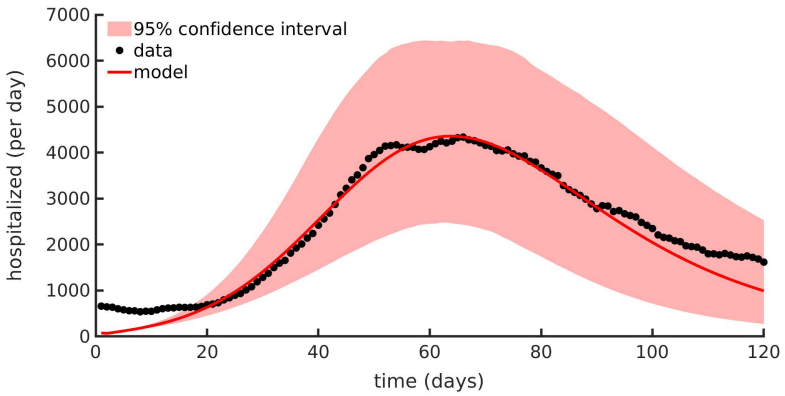

Figure 11. Figure represents model fitting (red line) with hospitalization data (black dots), and 95 % confidence interval (shaded region).

As depicted in Figure 12(a), our disclosure game model nicely captures the pattern of hospitalized cases, especially the peak timing and the duration of the outbreak. The goodness of fit (R^2) is approximately 0.95037, thus indicating our model's relatively strong predictive power. However, the model cannot reproduce the pattern in the data at the beginning and end of the outbreak. This is likely

because our model ignores comorbidity factors common during COVID-19 hospitalization. According to some statistics, it was observed that 75% of hospitalized patients with COVID-19 had at least one comorbidity. The most common among these were hypertension, diabetes, cancer, neurodegenerative diseases, cardiovascular diseases, obesity, and kidney diseases [33].

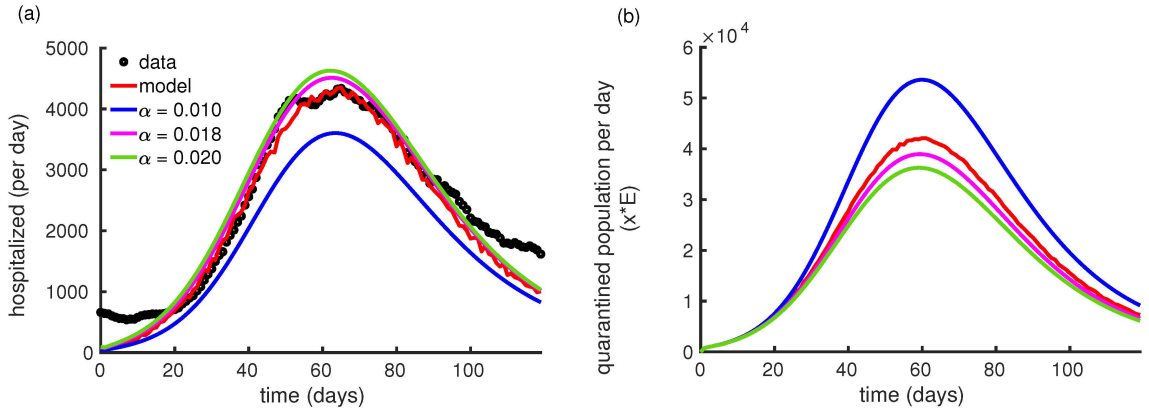

Figure 12. The dynamics of (a) model fit the confirmed new daily hospitalizations in Chile, South America, for the period from April to September 2020; (b) quarantined population per day with estimated parameters given in Θ_e and corresponding optimized values as shown in Table 3. The plots also show the scenarios of hospitalizations and quarantines for different values of the hospital admission rate α.

The estimated parameter values are given in Table 5. Along with these parameters, we also estimate the following initial conditions: $S(0) = 19623948.960, E(0) = 0, Q(0) = 0, I(0) = 8592.1279, H(0) = 11.509, R(0) = 0$, and $x(0) = 0.35805$. Additionally, we calculated the basic reproduction number R_0 with estimated parameters, which turned out to be 2.6876. Since this value is greater than 1, it signifies an active force of infection, thus leading to increased hospitalizations, which agrees with our model-fitting result. The detailed estimation method is given in the supplementary information. Moreover, we plotted the daily disclosing population with the estimated parameters, which estimates that around 45,000 individuals possibly took part in disclosing their infection and being quarantined during the peak timing of the outbreak (Figure 12(b)). To further examine this, we tested the different scenarios of the hospital admission rate (α) under the estimated parameters. A higher admission rate would imply a lower fraction of individuals left in the quarantine state, as seen in Figure 12(a),(b).

5. Discussion

The voluntary disclosure of infection and subsequent self-quarantine was a key recommendation from public health authorities during the emergence of COVID-19 to prevent community transmission. However, the effectiveness of this measure largely depends on individual decisions, which are influenced by the perceived costs associated with self-isolation. We investigated this decision-making approach by developing a standard susceptible-exposed-infected-recovered (SEIR) model, including hospital and quarantine compartments. We used a fractional derivative approach to represent the disease propagation within a population. We have shown that a rise in the rate of disease

transmission leads to an increase in the illness burden and the load placed on hospitals. Consequently, more individuals will be involved in the decision-making process. The concomitant impact of public health interventions and disease transmission rates will decrease the population's hospitalization rate, although it increases with the severity of the disease. Our research highlights that quarantine may be a favourable strategy at the individual level in specific epidemiological situations. This may provide insights for public health officials in developing intervention plans to control an epidemic.

There are recent works on game theory modelling social isolation behaviours and their impact on disease control [34, 35]. Our paper takes a distinct approach from these referenced works, although there is significant overlap in the motivations and applications. For instance, Hossein et al. [11] and Saad-Roy et al. [35] presumed that susceptible individuals are the players who can choose to adhere to non-pharmaceutical interventions (NPIs), while our model assumed that exposed individuals are the players in the game. Unlike the models of Hossein et al. [11] and Saad-Roy et al. [35], which assumed that susceptible individuals decide whether to adhere to NPIs, our model focused on the decision-making process of exposed individuals. This difference is crucial because it allows our model to directly link the availability of hospital beds to behavioural choices. In our framework, an increased healthcare capacity lowers the effective cost of disclosing an infection, thereby encouraging early self-quarantine. This mechanism improves the treatment outcomes and directly contributes to the reduction of disease transmission. Empirical results from our data fitting indicate that our approach more accurately reflects the observed epidemic dynamics, which provides a significant representation of the interplay between public health infrastructure and individual behaviours. For the same rationale, the fundamental disparity between our work and theirs lies in how we implement the control of infection transmission. Our approach focuses on reducing infection within the community by decreasing the number of infected individuals, while other papers primarily focus on depleting susceptible individuals from the population to achieve the same goal.

Evolutionary game theory has provided insightful perspectives on the evolution of behaviours during epidemics. Recently, it had applications in diverse emerging fields, thereby encompassing complex networks, biological physics, and cyberphysical systems. On the other hand, the fractional order technique has been used to model tumour growth, drug transport, immune response, and inflammation dynamics [36]. We conducted simulations across various fractional order values to compare the dynamical pattern generated by the fractional differential equation model with the ODE model. We compared them with traditional ODE simulations. Remarkably, as the fractional order (ζ) converges towards 1, the FDE results exhibit convergence with the ODE fit (Figure S3). Additionally, we found that the fractional-order derivative model fits the hospitalized data better than the ODE model (see Figure S4). Details are given in the supplementary information.

While the current research has furnished a valuable framework to understand the importance of quarantine as a strategy for controlling disease outbreaks, our model is based on simplified assumptions in many aspects. Our model does not incorporate asymptomatic infections. In our current formulation, exposed individuals immediately decide to quarantine based on the awareness of potential exposure. However, asymptomatic cases, which can comprise a substantial portion of infections, may remain undetected, thus delaying or precluding quarantine. This limitation could impact the model's applicability to scenarios where asymptomatic transmission is significant and can be addressed as a future direction. Moreover, there are more scopes for improvement in different directions. For example, one can consider the detailed framework to describe COVID-19

transmission, such as incorporating asymptomatic infections, severe infections, etc. Additionally, accounting for age-specific disease transmission processes or age-specific behaviours is more realistic [37]. Likewise, considering a networked population to incorporate quarantine will lead to a more significant understanding of the role of such containment measures in ongoing and future infection waves during an epidemic [38]. Furthermore, incorporating multiple infections and time delays in disease incubation can assist in capturing the dynamics of disease transmission in a more realistic way, especially COVID-like transmissions. From the perspective of epidemiological studies, it is also worthwhile to consider the impact of disease severity on infection or even look into infection-disclosing behaviours during the vaccine's availability. Coupling these ideas with the predictive abilities of fractional derivatives will be of great importance in managing disease outbreaks.

Nonetheless, our research provides a forum for discussing individuals' perceptions of disclosing infection at the start of an epidemic. Additionally, it explores the causes and consequences of an individual's strategic decision-making in the face of different epidemiological conditions. Individuals always maximize their payoff while ignoring population-level externalities when making such decisions. However, understanding the complex interaction is critical from a public health perspective because it may aid in disease outbreak management and benefit individual health in the community.

Appendix

Equilibria, Reproduction numbers and Stability analysis:

For our disease model (2.7), we have the disease-free equilibrium and the disease-endemic equilibrium. Depending on whether individuals opt for disclosing or not, there are mainly two important disease-free equilibria: $E_1^d = (N, 0, 0, 0, 0, 0)$ and $E_2^d = (0, 0, 0, 0, 0, 1)$. We call E_1^d a purely non-disclosing game and E_2^d a purely disclosing game. We compute the basic reproduction ratio, the control reproduction ratio, and the Jacobian matrix near the disease-free equilibrium E_1^d. This gives the optimal fraction of disclosing individuals needed to contain the disease soon.

Basic reproduction number R_0 when $x = 0$

In the case when $x = 0$, the reproduction number R_0 is given by the dominant eigenvalue of the next-generation method [39] as follows.

The infected classes for this system will be as follows:

$$ {}_0^C D_t^\zeta E(t) = \frac{\beta_s(I+E)S}{N} - \beta_e E, $$

$$ {}_0^C D_t^\zeta I(t) = \beta_e E - (1-\eta_q)\alpha I - \gamma I. $$

Now, we need to calculate f, v, F, and V, where f represents the vector of new infection rates, v represents the vector of transition rates (other than new infections) between compartments, and F and V are the Jacobian matrices of f and v, respectively. Therefore,

$$ f = \begin{bmatrix} \frac{\beta_s(I+E)S}{N} \\ 0 \end{bmatrix}, v = \begin{bmatrix} -\beta_e E \\ \beta_e E - \gamma I - (1-\eta_q)\alpha I \end{bmatrix}, $$

$$ F = \begin{bmatrix} \frac{\beta_s S}{N} & \frac{\beta_s S}{N} \\ 0 & 0 \end{bmatrix}, V = \begin{bmatrix} -\beta_e & 0 \\ \beta_e & -(\gamma + (1-\eta_q)\alpha) \end{bmatrix} $$

$$V^{-1} = \frac{1}{\beta_e\Big((1-\eta_q)\alpha+\gamma\Big)}\begin{bmatrix} -\Big(\gamma+(1-\eta_q)\alpha\Big) & 0 \\ -\beta_e & -\beta_e \end{bmatrix}$$

$$\implies FV^{-1} = \frac{1}{\beta_e\Big((1-\eta_q)\alpha+\gamma\Big)}\begin{bmatrix} \frac{-(\gamma+(1-\eta_q)\alpha)\beta_s S-\beta_e\beta_s S}{N} & \frac{-\beta_e\beta_s S}{N} \\ 0 & 0 \end{bmatrix}.$$

The dominant eigenvalue of the next-generation matrix $[FV^{-1}]$ is as follows:

$$R_0(S,N) = \frac{\beta_s S}{\beta_e N} + \frac{\beta_s S}{\Big((1-\eta_q)\alpha+\gamma\Big)N}.$$

Evaluating this at the disease-free equilibrium point
$E^{df}(S^{df}, E^{df}, I^{df}, Q^{df}, H^{df}) = (N, 0, 0, 0, 0)$ gives the reproduction number R_0 :

$$R_0 = \beta_S\left[\frac{1}{\beta_e} + \frac{1}{\Big((1-\eta_q)\alpha+\gamma\Big)}\right].$$

Control reproduction number R_c when $x \neq 0$

The control reproduction number R_c is obtained similarly and is computed as follows.
The Infected classes are as follows:

$${}_0^C D_t^{\zeta} E(t) = \frac{\beta_s(I+E)S}{N} - xE - \beta_e(1-x)E,$$

$${}_0^C D_t^{\zeta} I(t) = \beta_e(1-x)E - (1-\eta_q)\alpha I - \gamma I.$$

Therefore,

$$f = \begin{bmatrix} \frac{\beta_s(I+E)S}{N} \\ 0 \end{bmatrix}, v = \begin{bmatrix} -xE - \beta_e(1-x)E \\ \beta_e(1-x)E - \gamma I - (1-\eta_q)\alpha I \end{bmatrix},$$

$$F = \begin{bmatrix} \frac{\beta_s S}{N} & \frac{\beta_s S}{N} \\ 0 & 0 \end{bmatrix}, V = \begin{bmatrix} -x-\beta_e(1-x) & 0 \\ \beta_e(1-x) & -\Big((1-\eta_q)\alpha+\gamma\Big) \end{bmatrix},$$

$$\implies V^{-1} = \frac{1}{(x+\beta_e(1-x))\Big((1-\eta_q)\alpha+\gamma\Big)}\begin{bmatrix} -\Big(\gamma+(1-\eta_q)\alpha\Big) & 0 \\ -\beta_e(1-x) & -(x+\beta_e(1-x)) \end{bmatrix},$$

$$\implies FV^{-1} = \frac{1}{(x+\beta_e(1-x))\Big((1-\eta_q)\alpha+\gamma\Big)}\begin{bmatrix} \frac{-(\beta_s S)*((1-\eta_q)\alpha+\gamma)-\beta_e(1-x)\beta_s S}{N} & \frac{-(x+\beta_e(1-x))\beta_s S}{N} \\ 0 & 0 \end{bmatrix}.$$

Thus, the dominant eigenvalue of the next-generation matrix $[FV^{-1}]$ is as follows:

$$R_c(x) = \frac{\beta_s S}{(x+\beta_e(1-x))N} + \frac{\beta_e\beta_s(1-x)S}{(x+\beta_e(1-x))\Big((1-\eta_q)\alpha+\gamma\Big)N}.$$

Evaluating this at the disease-free equilibrium point E_1^d, gives the control-reproduction number R_c as a function of x:

$$R_c(x) = \frac{\beta_s}{(x+\beta_e(1-x))}\left[1 + \frac{\beta_e(1-x)}{\Big((1-\eta_q)\alpha+\gamma\Big)}\right].$$

The disease-free equilibrium is stable if $R_c < 1$, which implies the following:

$$x_c > \frac{\Big((1-\eta_q)\alpha+\gamma\Big)(\beta_s-\beta_e)+\beta_s\beta_e}{\beta_s\beta_e+(1-\beta_e)\Big((1-\eta_q)\alpha+\gamma\Big)}. \tag{A.1}$$

This indicates that it requires at least an x_c proportion of individuals to disclose their exposure to infection for the infection in the population to die out immediately.
Additionally, we compute the Jacobian matrix of the system at E_1^d:

$$J^d = \begin{bmatrix} \frac{-\beta_s(I+E)}{N} & \frac{-\beta_s S}{N} & 0 & \frac{-\beta_s S}{N} & 0 & 0 \\ \frac{\beta_s(I+E)}{N} & \frac{\beta_s S}{N} - x - \beta_e(1-x) & 0 & \frac{\beta_s S}{N} & 0 & -E+\beta_e E \\ 0 & x & -\eta_q\alpha-\gamma & 0 & 0 & E \\ 0 & \beta_e(1-x) & 0 & -(1-\eta_q)\alpha-\gamma & 0 & -\beta_e E \\ 0 & 0 & \eta_q\alpha & (1-\eta_q)\alpha & -\gamma_h-\mu_h & 0 \\ 0 & 0 & 0 & 0 & -\frac{\kappa a c_{nd} p_s x(1-x)}{(a+H)^2} & (1-2x)\kappa\Delta E \end{bmatrix}$$

Substituting the values of the equilibrium component into the Jacobian matrix, we get the following:

$$J^d = \begin{bmatrix} 0 & -\beta_s & 0 & -\beta_s & 0 & 0 \\ 0 & \beta_s-\beta_e & 0 & \beta_s & 0 & 0 \\ 0 & 0 & -\eta_q\alpha-\gamma & 0 & 0 & 0 \\ 0 & \beta_e & 0 & -(1-\eta_q)\alpha-\gamma & 0 & 0 \\ 0 & 0 & \eta_q\alpha & (1-\eta_q)\alpha & -\gamma_h-\mu_h & 0 \\ 0 & 0 & 0 & 0 & 0 & -\kappa c_d(1-\eta_q) \end{bmatrix}$$

It has the following eigenvalues:

$$\lambda_1 = 0,\ \lambda_2 = -\eta_q\alpha-\gamma,\ \lambda_3 = -\gamma_h-\mu_h,\ \lambda_4 = -kc_d(1-\eta_q)\ .$$

The other two eigenvalues are represented by the following quadratic equation in λ:

$$\lambda^2 - \lambda\Big[(\beta_s-\beta_e)-((1-\eta_q)\alpha+\gamma)\Big]+\Big[\beta_s\beta_e-(\beta_s-\beta_e)((1-\eta_q)\alpha+\gamma)\Big]=0.$$

The following sufficient criterion ensures that these eigenvalues are also negative:

$$\beta_s-\beta_e < min\{\sqrt{\beta_s\beta_e}, (1-\eta_q)\alpha+\gamma\}$$

However, this indicates the stability of the disease-free equilibrium E_1^d.

Use of AI tools declaration

The authors declare they have not used Artificial Intelligence (AI) tools in the creation of this article.

Acknowledgments

This work was initiated under the Shiv Nadar Institution of Eminence (SNIoE)'s Opportunity for Undergraduate Research (OUR) program. Viney Kumar thanks the Council of Scientific and Industrial Research (FILE NUMBER 09/1128(12030)/2021-EMR-I), India, for its financial support. All authors acknowledge SNIoE DST-FIST-funded computational lab support.

Conflict of interest

The authors declare there is no conflict of interest.

References

1. J. Huang, Y. Qian, Y. Yan, H. Liang, L. Zhao, Addressing hospital overwhelm during the COVID-19 pandemic by using a primary health care-based integrated health system: Modeling study, *JMIR Med. Inform.*, **12** (2024), 54355. https://doi.org/10.2196/54355
2. H. Lau, T. Khosrawipour, P. Kocbach, H. Ichii, J. Bania, V. Khosrawipour, Evaluating the massive underreporting and undertesting of COVID-19 cases in multiple global epicenters, *Pulmonology*, **27** (2021), 110–115. https://doi.org/10.1016/j.pulmoe.2020.05.015
3. Statista, Impact of coronavirus (COVID-19) on securing ICU beds in hospitals across India as of April 2021, 2021. Available from: https://www.statista.com/statistics/1231043/india-covid-19-impact-on-securing-icu-beds-in-hospitals/.
4. X. Wang, J. Wang, J. Shen, J. S. Ji, L. Pan, H. Liu, et al., Facilities for centralized isolation and quarantine for the observation and treatment of patients with COVID-19, *Engineering*, **7** (2021), 908–913. https://doi.org/10.1016/j.eng.2021.03.010
5. W. Zhu, M. Zhang, J. Pan, Y. Yao, W. Wang, Effects of prolonged incubation period and centralized quarantine on the COVID-19 outbreak in Shijiazhuang, China: A modeling study, *BMC Med.*, **19** (2021), 308. https://doi.org/10.1186/s12916-021-02178-z
6. A. Satapathi, N. K. Dhar, A. R. Hota, V. Srivastava, Coupled evolutionary behavioral and disease dynamics under reinfection risk, *IEEE Trans. Control Network Syst.*, **11** (2024), 795–807. https://doi.org/10.1109/TCNS.2023.3312250
7. S. Funk, M. Salathé, V. A. A. Jansen, Modelling the influence of human behaviour on the spread of infectious diseases: A review, *J. R. Soc. Interface*, **7** (2010), 1247–1256. https://doi.org/10.1098/rsif.2010.0142
8. M. Martcheva, N. Tuncer, C. N. Ngonghala, Effects of social-distancing on infectious disease dynamics: An evolutionary game theory and economic perspective, *J. Biol. Dyn.*, **15** (2021), 342–366. https://doi.org/10.1080/17513758.2021.1946177
9. M. Alam, J. Tanimoto, A game-theoretic modeling approach to comprehend the advantage of dynamic health interventions in limiting the transmission of multi-strain epidemics, *J. Appl. Math. Phys.*, **10** (2022), 3700–3748. https://doi.org/10.4236/jamp.2022.1012248
10. P. Premkumar, J. B. Chakrabarty, A. Rajeev, Impact of sustained lockdown during COVID-19 pandemic on behavioural dynamics through evolutionary game theoretic model, *Ann. Oper. Res.*, (2023). https://doi.org/10.1007/s10479-023-05743-2
11. H. Khazaei, K. Paarporn, A. Garcia, C. Eksin, Disease spread coupled with evolutionary social distancing dynamics can lead to growing oscillations, in *2021 60th IEEE Conference on Decision and Control (CDC)*, (2021), 4280–4286. https://doi.org/10.1109/CDC45484.2021.9683594
12. A. O. Yunus, M. O. Olayiwola, K. A. Adedokun, J. A. Adedeji, I. A. Alaje, Mathematical analysis of fractional-order caputo's derivative of coronavirus disease model via laplace adomian decomposition method, *Beni-Suef Univ. J. Basic Appl. Sci.*, **11** (2022), 144. https://doi.org/10.1186/s43088-022-00326-9

13. M. Wali, S. Arshad, J. Huang, Stability analysis of an axtended SEIR COVID-19 fractional model with vaccination efficiency, *Comput. Math. Methods Med.*, **2022** (2022), 3754051. https://doi.org/10.1155/2022/3754051
14. K. Oldham, J. Spanier, *The Fractional Calculus Theory and Applications of Differentiation and Integration to Arbitrary Order*, Elsevier, 1974.
15. H. M. Srivastava, Fractional-order derivatives and integrals: Introductory overview and recent developments, *Kyungpook Math. J.*, **60** (2020), 73–116. https://doi.org/10.5666/KMJ.2020.60.1.73
16. S. He, H. Wang, K. Sun, Solutions and memory effect of fractional-order chaotic system: A review, *Chin. Phys. B*, **31** (2022), 060501. https://doi.org/10.1088/1674-1056/ac43ae
17. M. R. Islam, A. Peace, D. Medina, T. Oraby, Integer versus fractional order SEIR deterministic and stochastic models of measles, *Int. J. Environ. Res. Public Health*, **17** (2020), 2014. https://doi.org/10.3390/ijerph17062014
18. C. T. Bauch, Imitation dynamics predict vaccinating behaviour, *Proc. R. Soc. B*, **272** (2005), 1669–1675. https://doi.org/10.1098/rspb.2005.3153
19. X. Wang, J. Wang, J. Shen, J. S. Ji, L. Pan, H. Liu, et al., Facilities for centralized isolation and quarantine for the observation and treatment of patients with COVID-19, *Engineering*, **7** (2021), 908–913. https://doi.org/10.1016/j.eng.2021.03.010
20. J. Hofbauer, K. Sigmund, *Evolutionary Games and Population Dynamics*, Cambridge University Press, 1998. https://doi.org/10.1017/CBO9781139173179
21. S. He, Y. Peng, K. Sun, SEIR modeling of the COVID-19 and its dynamics, *Nonlinear Dyn.*, **101** (2020), 1667–1680. https://doi.org/10.1007/s11071-020-05743-y
22. R. Niu, E. W. M. Wong, Y. Chan, M. A. V. Wyk, G. Chen, Modeling the COVID-19 pandemic using an SEIHR model with human migration, *IEEE Access*, **8** (2020), 195503–195514. https://doi.org/10.1109/ACCESS.2020.3032584
23. F. Ndaïrou, I. Area, J. J. Nieto, D. F. M. Torres, Mathematical modeling of COVID-19 transmission dynamics with a case study of Wuhan, *Chaos Solitons Fractals*, **135** (2020), 109846. https://doi.org/10.1016/j.chaos.2020.109846
24. H. Alrabaiah, M. Arfan, K. Shah, I. Mahariq, A. Ullah, A comparative study of spreading of novel corona virus disease by using fractional order modified SEIR model, *Alexandria Eng. J.*, **60** (2021), 573–585. https://doi.org/10.1016/j.aej.2020.09.036
25. S. Y. Chae, K. Lee, H. M. Lee, N. Jung, Q. A. Le, B. J. Mafwele, et al., Estimation of infection rate and predictions of disease spreading based on initial individuals infected with COVID-19, *Front. Phys.*, **8** (2020). https://doi.org/10.3389/fphy.2020.00311
26. H. Sun, Y. Qiu, H. Yan, Y. Huang, Y. Zhu, J. Gu, et al., Tracking reproductivity of COVID-19 epidemic in China with varying coefficient SIR model, *J. Data Sci.*, **18** (2020), 455–472. https://doi.org/10.6339/JDS.202007_18(3).0010
27. P. Ashcroft, S. Lehtinen, D. C. Angst, N. Low, S. Bonhoeffer, Quantifying the impact of quarantine duration on COVID-19 transmission, *Elife*, **10** (2021), 63704. https://doi.org/10.7554/eLife.63704
28. E. Mathieu, H. Ritchie, L. Rodés-Guirao, C. Appel, D. Gavrilov, C. Giattino, et al., COVID-19 Pandemic, 2020. Available from: https://ourworldindata.org/coronavirus.

29. S. Lumme, R. Sund, A. H. Leyland, I. Keskimäki, A Monte Carlo method to estimate the confidence intervals for the concentration index using aggregated population register data, *Health Serv. Outcomes Res. Method.*, **15** (2015), 82–98. https://doi.org/10.1007/s10742-015-0137-1
30. E. L. Ionides, C. Breto, J. Park, R. A. Smith, A. A. King, Monte Carlo profile confidence intervals for dynamic systems, *J. R. Soc. Interface*, **14** (2017), 20170126. https://doi.org/10.1098/rsif.2017.0126 .
31. B. Sen-Crowe, M. Sutherland, M. McKenney, A. Elkbuli, A closer look into global hospital beds capacity and resource shortages during the COVID-19 pandemic, *J. Surg. Res.*, **260** (2021), 56–63. https://doi.org/10.1016/j.jss.2020.11.062
32. P. Rzymski, N. Kasianchuk, D. Sikora, B. Poniedziałek, COVID-19 vaccinations and rates of infections, hospitalizations, ICU admissions, and deaths in Europe during SARS-CoV-2 omicron wave in the first quarter of 2022, *J. Med. Virol.*, **95** (2023), 28131. https://doi.org/10.1002/jmv.28131
33. R. Silaghi-Dumitrescu, I. Patrascu, M. Lehene, I. Bercea, Comorbidities of COVID-19 patients, *Medicina*, **59** (2023), 1393. https://doi.org/10.3390/medicina59081393
34. C. N. Ngonghala, P. Goel, D. Kutor, S. Bhattacharyya, Human choice to self-isolate in the face of the COVID-19 pandemic: A game dynamic modelling approach, *J. Theor. Biol.*, **32** (2020), 100397. https://doi.org/10.1016/j.jtbi.2021.110692
35. C. M. Saad-Roy, A. Traulsen, Dynamics in a behavioral-epidemiological model for individual adherence to a nonpharmaceutical intervention, *Proc. Natl. Acad. Sci.*, **120** (2023), 2311584120. https://doi.org/10.1073/pnas.2311584120
36. M. Farman, A. Akgül, A. Ahmad, S. Imtiaz, Analysis and dynamical behavior of fractional-order cancer model with vaccine strategy, *Math. Methods Appl. Sci.*, **43** (2020), 4871–4882. https://doi.org/10.1002/mma.6240
37. E. Addai, L. Zhang, J. K. K. Asamoah, J. F. Essel, A fractional order age-specific smoke epidemic model, *Appl. Math. Modell.*, **119** (2023), 99–118. https://doi.org/10.1016/j.apm.2023.02.019
38. J. Chen, C. Xia, M. Perc, The SIQRS propagation model with quarantine on simplicial complexes, *IEEE Trans. Comput. Soc. Syst.*, **11** (2024), 4267–4278. https://doi.org/10.1109/TCSS.2024.3351173
39. O. Diekmann, J. A. P. Heesterbeek, M. G. Roberts, The construction of next-generation matrices for compartmental epidemic models, *J. R. Soc. Interface*, **7** (2010), 873–885. https://doi.org/10.1098/rsif.2009.0386

AIMS Press